ROBUST HYBRID MOTION-FORCE CONTROL ALGORITHM FOR ROBOT MANIPULATORS

V. A. Mut, J. F. Postigo, R. O. Carelli and B. Kuchen

Instituto de Automatica, Universidad Nacional de San Juan
San Juan, Argentina, vmut@inaut.unsj.edu.ar

(Received: October 3, 1998 - Accepted: June 3, 1999)

Abstract In this paper we present a robust hybrid motion/force controller for rigid robot manipulators. The main contribution of this paper is that the proposed hybrid control system is able to accomplish motion objectives in free directions and force objectives in constrained directions under parametric uncertainty both in robot dynamics and stiffness constraint constant. Also, the given scheme is proved globally stable in the sense that the control objectives are achieved asymptotically, when a signum function is used in the control law, though giving rise to chattering effects. To avoid this problem a saturation function is used. In this case the motion and force errors are proved to be bounded functions. Using the proposed control structure there is no need to measure the derivative of the interaction forces. Some simulation results are given to illustrate the control system performance.

Key Words Robot Manipulators, Nonlinear Systems, Hybrid Motion-Force Control, Robust Control

»µoíÇ« S´ÇwRBQ¶°n ºBµn±U¿±P¼BÇ« nj °o¼Ç¯-S½oeËz i ³¯B£°j ¶k@@½ ¤oT@½ ð½ ³$B¸« Ë¼A nj **²k¼ña** ° j¼pCRB´] nj S½oe ²A¼kµA k¯Ä±U»« ºjB´®z¼Q ³¯B£°j ¤oT@½ ©Tv¼w ³½ SwA Ë¼A ³$B¸« Ë¼A ¶k ª î ©´w /j±{»« ¼n ²k{ j°kd« »¸{ S¶BY n¼k¸« nj ©µ RB¶°n ºB´ñ¼«B@¼j nj ©µ ºoT«¼nBQ ËÅª¤«B¯ £½o{ nj k¼Ø RB´] nj °o¼¯ ² A¼kµA j°n nB½ ³¶ ¤oT@½ é¶BU nj ¨±®¢¼w é¶BU ð½ ³½ »«B¢®µ SwA ²k{ S¶BY ³½ B\¯Cp¼ Ë¼®`ªµ /jpBw ²jn°C o¶ é¶BU ð½ p¼³¦Åv« Ë¼A p¼ºo½£±¦] º¼o¶ /j±{»« n¼k½BQ Â½©Tv¼w k¯Ä²k{ ¥æBe K¯B\« S$Be ³¶ ¬k¼wn B¶ ¤oT@½¿ B¶ /k¯±{»« ¥½kLU n¼k¯o½ é¶M±U ³¶ °o¼¯ ° S½oe ºBµB¤i S$Be Ë¼A nj ³½ j±{»« S¶BY /j±{»« ²jB´TwA ªBL{A ©Tv¼w jo½nB½ y ½Bª¯ º¼o¶ /Sv¼¯ y z½©µo¶ ºBµ°o¼¯ ·Tz« ºo¼£¿²p¼k¯Ä ³¶ ºpB¼¯ ,¤oT@½ nBT i Bw Ë¼A p¼²jB´TwA /SwA ²k{ ³Å¼nA ºpBw ³¼L{ jn±« k®a [½BT¯ ¤oT@½¿

INTRODUCTION

Control of robotic manipulators can be classified into two different approaches: motion control and constrained motion control. Motion Control is used when the robot arm moves in a free space without interacting with the environment. Motion control specifications are given in terms of a desired motion trajectory. On the other hand, Constrained Motion Control of robots is concerned with the control of robots whose end-effector interacts mechanically with the environment, which leads to control schemes that regulate the interaction forces between the end-effector and the environment [1]. Most assembly operations and manufacturing tasks require mechanical interactions with the environment or with the object being manipulated, along with fast motion in free and unconstrained space. Several controller schemes have been proposed in the literature and can basically be classified as compliant motion control, pure force control, and hybrid motion-force control [2,3].

The dynamic behaviour of rigid manipulators can be modelled by a set of complex nonlinear differential equations. Most high performance model-based control schemes rely on the exact

cancellation of the nonlinear dynamics. The uncertainty in some robot parameters, as link inetria and payload, normally degrades the control performance. In this context, there exist two basic approaches to reduce the effects of uncertainties: adaptive robot control and robust robot control [15,16]. Adaptive controllers for motion and constrained motion robots have been proposed in the literature [4,5,6,7]. Regarding the robust control approach, there exist some schemes with global stability demonstrations to solve the motion control problem [8,9], and a robust adaptive motion - force controller [10].

In this paper, we present a robust hybrid motion-force controller for robot manipulators as an extension of the robust motion controller in [9], using the hybrid controller structure described in a previous work [7]. The controller has a simple structure as a result of being based upon robot model parameterization and the use of switching functions. The controller is robust to uncertainties both in the manipulator dynamics and the environment stiffness. This approach does not require measurement of the joint acceleration or the force derivative. A global stability demonstration is given based on Lyapunov analysis, without any linearization assumptions. Also, boundedness of control errors is proved when a saturation function is used to avoid chattering.

The paper is organized as follows. In section II we summarize the manipulator model. Section III presents the problem formulation. The proposed robust hybrid controller is given in section IV. In section V we describe some simulation results, and finally in section VI the concluding remarks are given.

ROBOT MODEL

In the absence of friction and other disturbances, the Cartesian-space dynamics of an n-link constrained rigid robot manipulator can be written as,

$$H(x)\ddot{x} + C(x,\dot{x})\dot{x} + G(x) + F = J^{-T}t \qquad (2.1)$$

where x is the nxl vector of Cartesian position and Euler angles of the manipulator end-effector, in a reference frame R_0 fixed to the robot base; t is the nxl vector of torques (or forces) applied to the robot joints by the actuators; H(x) is the nxn symmetric positive definite manipulator inertia matrix, $C(x,\dot{x})\dot{x}$ is the nxl vector of centripetal and Coriolis forces, G(x) is the nxl vector of gravitational forces; J(q) is the nxn manipulator Jacobian matrix, assumed to be nonsingular, q is the nxl vector of joint displacements and F is the nxl vector of interaction force/moments at the end-effector. In case J be singular due to arm singularities or J be non-square due to arm redundancy, it is necessary to apply the generalized inverse based on the singular value decomposition theorem, so that the null space existing in Cartesian space or joint space can be separated. The manipulator described by Equation 2.1 is assumed non-redundant. It is assumed that the robot is equipped with joint position and velocity sensors and a force sensor at its end-effector. Although the motion Equation 2.1 is complex, it has several fundamental properties which can be used to ease the control system. The properties are as follows:

Property 1 (See[4]). By using a proper definition of matrix $C(x,\dot{x})$ (only the vector $C(x,\dot{x})\dot{x}$ is uniquely defined), matrices H(x) and $C(x,\dot{x})$ in Equation 2.1 satisfy

$$Z^T [dH(x)/dt - 2C(x,\dot{x})] z = O \qquad \forall z \in R^n$$

Property 2 (See[4]). A part of the dynamic structure 2.1 is linear in terms of a suitable selected set of robot and load parametes, i.e.

$$H(x)\ddot{x} + C(x,\dot{x})\dot{x} + G(x) = W(x,\dot{x},\ddot{x})q \qquad (2.2)$$

Where $W(x,\dot{x},\ddot{x})$ is an nxm matrix and q is an mxl vector containing the robot and load parameters.

Property 3 (See [6]). H(x) is an nxn symmetric positive definite matrix and there is a constant $a>0$ such that

$aI \le H(x) \quad \forall x \in R^n$

For revolute joint robots if, in addition, $J^{-1}(q)$ is a bounded nxn matrix, then there is a $b (a<b<\infty)$ such that,

$aI \le H(x) \le bI \quad \forall x \in R^n$

PROBLEM FORMULATION

Following Raibert and Craig [3] and Slotine and Li [4] two coordinate systems are defined. The first one-already defined in section II- is a frame of reference R_0 fixed on the robot base, which defines a Cartesian space called operational space. In this space, the end-effector configuration is represented by using a vector x, composed of the Cartesian position and Euler angles of the end-effector. The second is the compliance frame R_c (also called constraint frame), which is used to describe the compliant motion task. It is naturally defined by the so called natural constraints, so that the coordinates be associated to the unconstrained and the constrained directions in the task space. Without loss of generality, we assume that both coordinate frames R_0 and R_c have the same origin. In general, the R_c frame may be time-varying. Task specifications can now be given in the compliance frame: motion specifications in the free directions and force specifications in the constrained directions.

We digress momentarily to establish some nomenclature used henceforth. Vectors $x, \dot{x}, \ddot{x}$ are respectively the position, velocity and acceleration of the end-effector specified in the frame R_0. F is the interaction force between the environment and the end-effector specified in the same frame R_0. Note that here "position" means both position and orientation, and "force" implies both force and torque. In the compliance frame R_c, position, velocity and acceleration are expressed by x_c , $\dot{x}_c$, $\ddot{x}_c$ respectively and force by F_c . Position and force reference trajectories specified in the same frame are given by x_{cd}, $\dot{x}_{cd}$, $\ddot{x}_{cd}$, F_{cd}, $\dot{F}_{cd}$, $\ddot{F}_{cd}$. The forthcoming analysis needs a transformation matrix $R \in R^{nxn}$ between compliance and operational coordinates. This matrix, a rotation matrix, is defined by the interaction task surface and is given by the task planner. In general $R = R(t)$ is time-varying, R and $\dot{R}$ are assumed bounded and R has its minimum singular value bounded away from zero (thus implying that $R^{-1} = R^T$ is bounded). Besides, $\dot{R}^T$ and $\ddot{R}^T$ exist and are assumed bounded, too. Conditions on the derivatives are naturally satisfied for smooth task surfaces. Therefore, the following relations hold:

$$
\begin{aligned}
x_c &= R^T(t)x \\
\dot{x}_c &= \dot{R}^T(t)x + R^T(t)\dot{x} \\
\ddot{x}_c &= \ddot{R}^T(t)x + 2\dot{R}^T(t)\dot{x} + R^T(t)\ddot{x} \qquad (3.1) \\
F_c &= R^T(t)F \\
\dot{F}_c &= \dot{R}^T(t)F + R^T(t)\dot{F}
\end{aligned}
$$

For the problem formulation, R(t) is assumed to be known. A constant compliance selection matrix $S=\text{diag}_{(nxn)}\{s_i\}$ specifies which coordinates in R_c are under force control (indicated by $s_i = 0$), and which ones are under motion control (indicated by $s_i = 1$). Matrix S premultiplied by a vector in compliance coordinates, preserves the unconstrained coordinate components and zeroes the others. A complementary effect is obtained with the matrix $S' = (I_n - S)$, where I_n represents the identity nxn matrix.

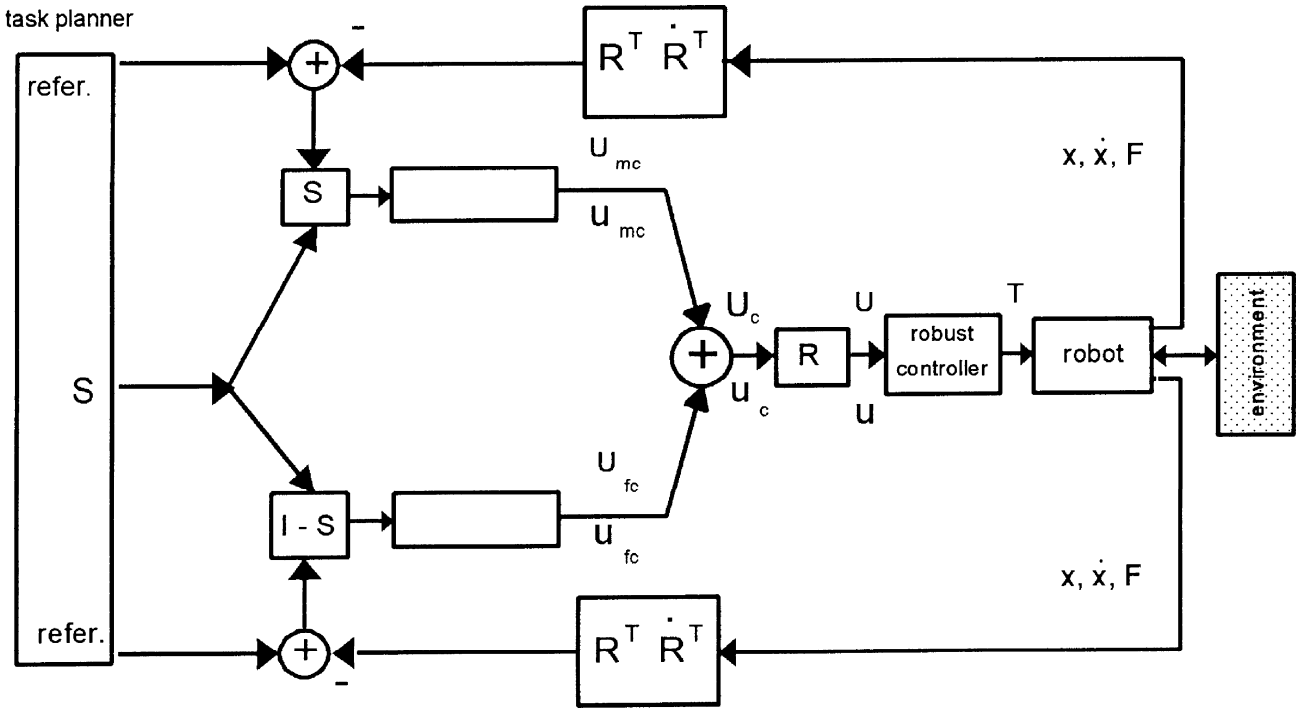

Figure 1. Control structure.

The manipulator is assumed to be equipped with a force sensor at its end-effector. Now it is necessary to consider the interaction model which generates reaction forces. The environment is modelled by a stiffness matrix K_e as,

$$F_c = K_e [x - x_e]_c = K_e [x_c - x_{ec}] \quad (3.2)$$

with $x_{ec}(t)$ the position of the constraint point which is currently interacting with the end - effector. In this paper we consider a static environment, so $\dot{x}_{ec} = 0$. K_e is assumed to be uncertain but constant. Likewise, we could also consider a rigid environment, for instance, the parts assembly and polish applications. Here, a compliance model with stiffness matrix is then associated with the force sensor.

We are now ready to formulate the robust motion/force control problem. Let us consider the manipulator described by Equation 2.1. The parameter vector q -from properties of [4]- of the manipulator, payload and environment is constant but unknown. The robot Jacobian matrix J(q) is assumed to be non-singular and known. Knowledge of J(q) is not restrictive because it does not depend on the dynamic parameters. The hybrid motion/force control specifications are given in terms of a desired motion trajectory $x_{cd}(t)$ in the unconstrained directions and a desired force trajectory $F_{cd}(t)$ in the constrained directions.

The robust hybrid control problem can be stated as that of designing a control law to compute the joint applied torques t, so that the following objectives be verified:

a) $S(x_{cd}(t) - x_c(t)) \to 0$ as $t \to \infty$ in the unconstrained directions, and

b) $S'(F_{cd}(t) - F_c(t)) \to 0$ as $t \to \infty$ in the constrained directions.

ROBUST HYBRID CONTROLLER

Robust Controller. Let us consider the control structure of Figure 1 [7]. There, we recognize two independent feedback loops: one for controlling motion in the unconstrained

coordinates of the compliance frame R_c, and the other for controlling force in the constrained coordinates.

A motion/force controller based on the structure given in [7] with estimated values of the robot dynamic model is,

$$J^{-T}t = H_0 [u - R\ddot{R}^T x - 2R\dot{R}^T \dot{x} - \dot{R}R^T v] + C_0[\dot{x}-n] + G_0 + F \quad (4.1)$$

where H_0, C_0, G_0 have the same functional forms as H(x), C (x) and G(x) respectively, with estimated dynamic parameters. The signal vectors u and v are related to the corresponding vectors expressed in the compliance frame R_c by the transformation R as,

$$u = R(t)\, u_c \; ; \; n = R(t)\, n_c \quad (4.2)$$

where u_c and n_c are obtained from the motion and force control loop components (see Figure 1) as,

$$u_c = u_{mc} + u_{fc} \; ; \; n_c = n_{mc} + n_{fc}. \quad (4.3)$$

where n_{mc} and n_{fc}, u_{mc} and u_{fc} are orthogonal, respectively.

Vectors u_{mc}, n_{mc} are defined as,

$$n_{mc} = \ddot{x}_{cd} + M_m^{-1} [B_m \dot{e}_{xc} + K_m e_{xc}] \quad (4.4)$$

$$n_{mc} = -[l/(r + l)]\, M_m^{-1} [M_m \ddot{e}_{xc} + B_m \dot{e}_{xc} + K_m e_{xc}] \quad (4.5)$$

Likewise, vectors u_{fc}, n_{fc} are calculated as,

$$u_{fc} = S' K_e^{-1} [\ddot{F}_{cd} + M_f^{-1} (B_f \dot{e}_{fc} + K_f e_{fc})] \quad (4.6)$$

$$n_{fc} = -[l/(r + l)]\, S' K_e^{-1} M_f^{-1} [M_f \ddot{e}_{fc} + B_f \dot{e}_{fc} + K_f e_{fc}] \quad (4.7)$$

In Equations 4.3-4.7, $e_{xc} = S(x_{cd} - x_c)$ and $e_{fc} = S'(F_{cd} - F_c)$ are the position and force errors respectively expressed in the compliance frame. Also, $S' = I_n - S$, $r = d(.)/dt$, l is a positive design scalar and M_m, B_m, K_m, M_f, B_f, K_f are $n \times n$ positive definite and diagonal design matrices. Note that x_c, $\dot{x}_c$, F_c, $\dot{F}_c$ are obtained from measured values of q, $\dot{q}$ and F by using the relation $x = f(q)$ between x and q, and Equations 3.1 and 3.2.

Remark 1. Vectors n_{mc} and n_{fc} in Equations 4.5 and 4.7 can be written as,

$$n_{mc} = -[r/(r+ l)]\, \dot{e}_{xc} - [l/(r + l)]\, M_m^{-1} (B_m \dot{e}_{xc} + K_m e_{xc})$$

$$n_{fc} = -[r/(r + l)] S' K_e^{-1} \dot{e}_{fc} - [l/(r + l)] S' K_e^{-1} M_e^{-1} (B_f e_{fc} + K_f e_{fc}) \quad (4.8)$$

The above expressions and Equation 4.1 clearly show that the computation of t requires knowledge of end-effector position x, velocity $\dot{x}$, force F and its derivative $\dot{F}$ (no measurement of acceleration $\ddot{x}$ and second derivative of force $\ddot{F}$ is required).

Remark 2. To avoid measuring $\dot{F}$, $\dot{F}_c$ in Equations 4.6 and 4.8 can be computed as

$$\dot{F}_c = K_e(\dot{x}_c - \dot{x}_{ec}). \quad (4.9)$$

Remark 3. Vectors n_{mc} and n_{mc} defined in Equations 4.4 and 4.5 have components corresponding only to the unconstrained task space coordinates and vectors u_{fc} and n_{fc} in Equations 4.6 and 4.7 have components only in the constrained coordinates. This comes from using selection matrices S and S' which select the components of the motion and force controlled directions respectively. Consequently, u_{mc}, u_{fc} as well as n_{mc}, n_{fc} represent a partition of u_c and v_c respectively in Equation 4.3.

Now, considering Equation 4.6 and Remark 2, we can write

$$u_{fc} = S' K^{-1}_e \ddot{F}_{cd} + S' K^{-1}_e M^{-1}_f B_f S' K_e (\dot{x}_{cd} - \dot{x}_c) + S' K_e^{-1} M^{-1}_f K_f e_{fc}$$

$$u_{fc} = K_{e1} \ddot{F}_{cd} + K_{e2} (\dot{x}_{cd} - \dot{x}_c) + K_{e3}\, e_{fc} \quad (4.10)$$

where

$$K_{e1} = S' K_e^{-1}$$

$$K_{e2} = S' K_e^{-1} M_f^{-1} B_f S' K_e$$

$$K_{e3} = S' K_e^{-1} M_f^{-1} K_f$$

Likewise, considering Equation 4.7, Remark 1 and Remark 2 yield,

$$n_{fc} = -[l/(r+ l)] S' K_e^{-1} \ddot{e}_{fc} + [-1/(r+ l)] S' K_e^{-1}$$

$$M_f^{-1}(B_f\dot{e}_{fc} + K_f e_{fc})$$

$$\eta_{fc} = [r/(r+l)]\, S' K_e^{-1} S' K_e (\dot{x}_{cd} - \dot{x}_c) - [r/(r+l)]\, S' K_e^{-1} M_f^{-1} B_f e_{fc} - [l/(r+l)]\, S' K_e^{-1} M_f^{-1} K_f e_{fc}$$

$$v_{fc} = -[r/(r+l)]K_{e4}(\dot{x}_{cd} - \dot{x}_c) - [r/(r+l)]K_{e5}e_{fc} - [l/(r+l)]K_{e6}e_{fc} \quad (4.11)$$

where:

$$K_{e4} = S' K_e^{-1} S' K_e$$
$$K_{e5} = S' K_e^{-1} M_f^{-1} B_f$$
$$K_{e6} = S' K_e^{-1} M_f^{-1} K_f$$

Now, based on control law Equation 4.1, properties of [4] and Equations 4.10 and 4.11 with parameterization of u and v signals in terms of K_e, we propose the following motion/force control law

$$J^{-T}\tau = f(x, \dot{x}, x_{cd}, \dot{x}_{cd}, \ddot{x}_{cd}, F, F_{cd}, \dot{F}_{cd}, \ddot{F}_{cd}, R, \dot{R}^T, \ddot{R}^T)\, q_0 + F \quad (4.12)$$

where $f \in R^{nxm}$ is a signal matrix and $q_0 \in Rm$ is the uncertain robot and stiffness parameters vector. In Equation 4.12, τ represents the control actions, i.e. the torques/forces to be applied to the robot joints.

Now, based on control law Equation 4.12, we propose the following robust motion/force control law,

$$J^{-T}\tau = f(x, \dot{x}, x_{cd}, \dot{x}_{cd}, \ddot{x}_{cd}, F, F_{cd}, \dot{F}_{cd}, \ddot{F}_{cd}, R, \dot{R}^T, \ddot{R}^T)\, q_0 - f(.)\, K\, \mathrm{sign}(f^T(.)\, \eta) + F \quad (4.13)$$

where K is a constant nxm matrix to be defined in IV.3. This control law has a similar structure to that of [9] for pure motion robot control.

Error Model Before carrying out the stability analysis, it is necessary to obtain the so called error model [11], which relates dynamically the signal vector v and the parameter error vector $\tilde{q} = q_0 - q$. By equating robot model of Equation 2.1 and the control law of Equation 4.13, we obtain

$$H\ddot{x} + C\dot{X} + G + F = f q_0 - f K\, \mathrm{sign}(f^T\eta) + F \quad (4.14)$$

Now, by substituting $q_0 = \tilde{q} + q$ into Equation 4.14 and observing from Equations 4.12 and 4.1 that,

$$f q = H[u - R\ddot{R}^T x - 2R\dot{R}^T \dot{x} - \dot{R}\eta_c] + C[\dot{x} - \eta] + G$$

the closed loop Equation 4.14 results

$$H(\ddot{x} - \ddot{u}') + H\dot{R}\eta_c + C\eta = f\tilde{q} - f K\, \mathrm{sign}(f^T\eta) \quad (4.15)$$

with

$$u' = u - R\ddot{R}^T x - 2R\dot{R}^T \dot{x}.$$

The evaluation of $(\ddot{x} - \ddot{u}')$ now follows,

$$(\ddot{x} - \ddot{u}') = RR^T(\ddot{x} - \ddot{u}')$$

where

$$R^T(\ddot{x} - \ddot{u}') = R^T\ddot{x} - R^T u + \ddot{R}^T x + 2\dot{R}^T \dot{x}.$$

But, from Equations 3.1 and 4.2,

$$R^T(\ddot{x} - \ddot{u}') = \ddot{x}_c - u_c.$$

Now consider the following partitions in free and constrained directions

$$\ddot{x}_c = \ddot{x}_{mc} + \ddot{x}_{fc} \quad ; \quad u_c = u_{mc} + u_{fc}$$

with

$$\ddot{x}_{mc} = S\ddot{x}_c \quad ; \quad \ddot{x}_{fc} = S'\ddot{x}_c.$$

Then,

$$R^T(\ddot{x} - \ddot{u}') = \ddot{x}_c - u_c = (\ddot{x}_{mc} - u_{mc}) + (\ddot{x}_{fc} - u_{fc}). \quad (4.16)$$

Manipulating Equations 4.4 - 4.5, 4.6 - 4.7 and the stiffness model of Equation 3.3, yields

$$\ddot{x}_{mc} - u_{mc} = \dot{\eta}_{mc} + l\eta_{mc} \; ; \; \ddot{x}_{fc} - u_{fc} = \dot{\eta}_{fc} + l\eta_{fc}$$

Then, Equation 4.16 can be written as

$$R^T(\ddot{x} - \ddot{u}') = (\dot{\eta}_{mc} + \dot{\eta}_{fc}) + l(\eta_{mc} + \eta_{fc})$$

and considering vector partition of Equation 4.3

$$R^T(\ddot{x} - \ddot{u}') = \dot{\eta}_c + l\eta_c.$$

Now, from Equation 4.2 and

$$\eta = R(t)\,\eta_c \quad ; \quad \dot{\eta} = \dot{R}(t)\,\eta_c + R(t)\,\dot{\eta}_c$$

it results,

$(\dot{x}-\dot{u}')=RR^T(\dot{x}-\dot{u}')=R(\eta_c+\lambda\eta_c)=\eta+\lambda\eta-R\eta_c$.
Going back to Equation 4.15, we obtain

$$H(\dot{\eta}+\lambda\eta)+C\eta=f_q-f_K\,\mathrm{sign}(f^T\eta) \quad (4.17)$$

Equation 4.17 describes the so called error model equation.

Main Results Now we state the main properties of the proposed robust controller in the following proposition.

Proposition 1. Considering the control law Equation 4.13 in closed loop with the manipulator Equation 2.1, the following holds,

a) $\eta \in L_2^n \cap L_\infty^n$

b) $\eta_{mc}, \eta_{fc} \in L_2^n \cap L_\infty^n$

c) $e_{xc}, \dot{e}_{xc} \in L_2^n \cap L_\infty^n$, $e_{xc} \to 0$ as $t \to \infty$

d) $e_{fc}, \dot{e}_{fc} \in L_2^n \cap L_\infty^n$, $e_{fc} \to 0$ as $t \to \infty$. ê ê ê

We note that c) and d) in proposition 1 ensure that the control objectives of Equations 3.4 and 3.5 are verified.

Proof. Consider the error model of Equation 4.17, and the following non negative function of time (remember property 3),

$$V(t) = 1/2[\eta^T H \eta] \quad (4.18)$$

whose time derivative along the trajectories of Equation 4.17 is,

$$\dot{V} = -\lambda\eta^T H \eta + \eta^T f_q - \eta^T f_K\,\mathrm{sign}(f^T\eta) \quad (4.19)$$

Where we have used the property 1 to eliminate the term $\eta^T(1/2\dot{H}-C)\eta$.

Taking $K = \mathrm{diag}(k_i)$ with $K_i > \bar{q}_i$, then $\dot{V}$ in Equation 4.19 satisfies $V(t) > 0$. This implies that $\eta \in L_\infty^n$. Also H is lower bounded as established by property 3. Then integrating Equation 4.19 from 0 to T and considering T in the limit, it verifies that $\eta \in L_2^n$. This establishes a).

Now, from Equation 4.3 and Remark 3, we can write the following vector partition,

$$R^T(t)\,\eta = \eta_c = \eta_{mc} + \eta_{fc}$$

and recalling that R was assumed to be bounded, from a) we immediately conclude b). Finally, as $\eta_{mc}, \eta_{fc} \in L_2^n \cap L_\infty^n$, from Equations 4.5, 4.7 and lemma shown in Desoer and Vidyasagar (1975), pp. 59 [13], we derive c) and d). ê ê ê

Remark 4 The control law of Equation 4.1 contains the signum function. As a result we might expect ``chattering'' to occur. In order to alleviate this situation, we can replace the signum function by the mxl vector of the saturation function $\mathrm{sat}\,\eta = (\mathrm{sat}(\eta_1), \ldots, \mathrm{sat}(\eta_i), \ldots, \mathrm{sat}(\eta_m))^T$, defined as,

$$\mathrm{sat}(\eta_i) = \begin{cases} 1 & \eta_i > 1 \\ \eta_i & -1 < \eta_i < 1 \\ -1 & \eta_i < -1 \end{cases} \quad (4.20)$$

where η_i are the components of the mxl vector $\eta = f^T n/\varepsilon$, with i= 1, ..., m and $\varepsilon > 0$, and η_i containing the bounds for the commuting switching planes [12]. By using the saturation function, the convergence of the control errors can not be concluded towards zero but to their bounds.

Proposition 2. Consider the control law

$$J^T\tau = f(x,\dot{x},x_{cd},\dot{x}_{cd},\ddot{x}_{cd},F,F_{cd},\dot{F}_{cd},\ddot{F}_{cd},\dot{R},R^T,\ddot{R}^T)q_0 - f(.)\,K\,\mathrm{sat}[(f^T(.)\eta)/\varepsilon] + F \quad (4.21)$$

where sat(.) is defined in Equation 4.20. Then, the control errors are ultimately bounded.

Proof. Consider the error model of Equation 4.17, where sign(.) is substituted by sat(.), and the following non negative time function (remember property 3),

$$\dot{V}(t) = 1/2[\eta^T H \eta] \quad (4.22)$$

whose time derivative along the trajectories of the error equation is

$$\dot{V} = -\lambda\eta^T H \eta = \eta^T f_{\tilde{q}} - \eta^T f_K\,\mathrm{sat}\left(\frac{f^T\eta}{\varepsilon}\right) \quad (4.23)$$

When $\mathrm{sat}(\eta_i) = \eta_i$ we can rewirte Equation 4.23 as

$$\dot{V} = -\alpha V + \eta^T f_{(\tilde{q}+u)} \quad (4.24)$$

where $\alpha = 2\lambda$ and $u = -\dfrac{K f^T\eta}{\varepsilon}$.

By inspecting the second term of Equation 4.24 and recalling $K = diag(K_i)$ with $K_i \geq \eta_i$ it follows

$$n^T f[\tilde{q} + u] \leq n^T f[K\, sign(f^T n) - \frac{K f^T n}{e}] = n^T f K [sign(f^T n) - \frac{f^T n}{e}] \quad (4.25)$$

$$n^T f[\tilde{q} + u] \leq n^T f[K\, sign(f^T n) - \frac{K f^T n}{e}] \leq \| n^T f \| \lambda_{max}(K)[\rho(m) - \frac{\| (f^T n) \|}{e}]$$

The function defined in Equation 4.25 has a maximum for:

$$\| f^T n \| = (\rho \bar{m} \frac{e}{2})$$

Whose value is

$$[m \lambda_{max}(K) \frac{e}{4}]. \quad (4.26)$$

By substituting Equation 4.26 into Equation 4.24 we obtain

$$\dot{V} \leq -aV + r \quad (4.27)$$

where $r = [m \lambda_{max}(K) \frac{e}{4}]$.

Considering Equation 4.27 it is clear that, V(t) is ultimately bounded by r/a. (4.28)

From Equation 4.22 it holds

$$V \geq \frac{1}{2} g(H) \| v \|^2 \quad (4.29)$$

where $g(H) = \inf_q(\lambda_{min}(H))$.

From Equations 4.27 and 4.28 we conclude that $\| v \|^2$ is ultimately bounded by $2r/ag$ (H). Remembering that $v = R v_{mc} + R v_{fc}$, then the bounds of v_{mc} and v_{fc} are established from the bounds on v. Now, considering the $\| . \|$ of the filtering operators given by Equations 4.5 and 4.7, we obtain the bounds of motion and force errors, i.e.,

$$\| e_{mc} \| \leq b_1 \| \eta_{mc} \|$$

$$\text{with } b_1 = \frac{4e^{-1}}{m_m^{-1} b_m} + \frac{1}{m_m^{-1} k_m}$$

$$\| \dot{e}_{mc} \| \leq b_2 \| v_{mc} \|$$

$$\text{with } b_2 = 1 + \frac{4 e^{-1}}{m_m^{-1} b_m} \quad (4.30)$$

$$\| e_{fc} \| \leq b_3 \| K_e \eta_{fc} \|$$

$$\text{with } b_3 = \frac{4e^{-1}}{m_f^{-1} b_f} + \frac{1}{m_f^{-1} K_f}$$

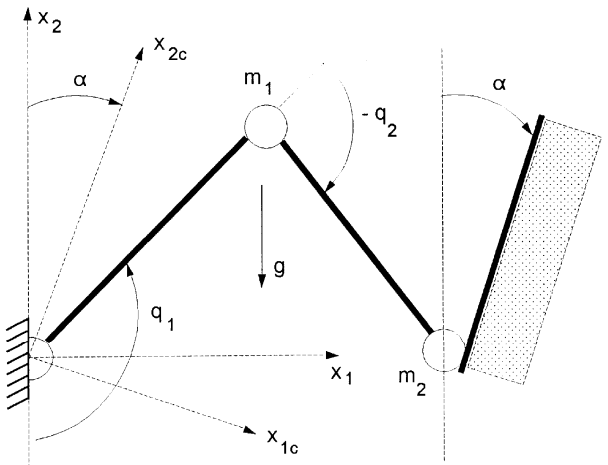

Figure 2. Two link manipulator and its environment.

For the case $K_e = diag(k_e)$ is verified that $\| e_{fc} \| \leq b_3 k_e \| \eta_{fc} \|$.

SIMULATION RESULTS

Computer simulations have been carried out to show the performance of the proposed robust controller. The manipulator used for the simulations is a two degree of freedom arm in a vertical plane, in contact with its environment as shown in Figure 2.

In this particular case R is a constant matrix given by,

$$R = \begin{bmatrix} \cos\alpha & \sin\alpha \\ -\sin\alpha & \cos\alpha \end{bmatrix}; \text{ with } \alpha = 0.$$

Selection matrix is specified as S = diag [0, 1].

The manipulator is modeled as two rigid links of unitary length with masses m_1 and m_2 at the distal ends of the links. Friction is not considered in the model.

Scalar g is the gravity acceleration magnitude. Numerical values of the parameters are m_1=4 kg, m_2=2 kg and K_e=1000 N/m. It is assumed that m_1, m_2, and K_e are uncertainly known.

From Equation 4.1, the vector control law can be written as,

$$t = J^T f q_0 + J^T f K\, sign(f^T v) + J^T F = f q_0 + f K\, sign(f^T J^{-T} \eta) + J^T F \quad (5.1)$$

where the uncertain parameter vector, taken as $q_0 = [q_{10}\ q_{20}\ q_{30}\ q_{40}]^T =$
$[3 \quad 0.00375 \quad 1 \quad 0.00125]^T$
is an estimation of:
$q = [m_1\ m_1/k_e\ m_2\ m_2/k_e]^T$. We must note that in Equation 5.1, $f = J^T f$, and $K = \text{diag}\,[k_1, k_2, k_3, k_4]$.

Motion trajectory along the constraint surface is specified as,
$x_{cd}(t)=(x_{cd1},x_{cd2})^T= [0,0.5+0.2\ \cos(\frac{p}{2}t)]^T$ [m]
and force normal to the constraint surface is specified as
$f_{cd}(t) = (f_{cd1}, f_{cd2})^T = [1 + 0.5 \cos(\frac{p}{2}t),0]^T$ [N]

Simulation is carried out using the following design parameters (see Equations 4.5 and 4.7):
M_m= diag [1], B_m= diag [10], K_m= diag [25], M_f= diag [1], B_f= diag [10], K_f= diag[250], l=30.

In the first simulation we consider the signum function in the control law. Figure 3 shows the evolution of force error e_{fc1} in the constrained direction and the evolution of motion error e_{xc2} in the unconstrained direction. For this case, torques t_1, t_2 are shown in Figure 4. Note that motion and force errors converge to zero, but there is chattering in the torques applied to the joints.

In the second simulation, we consider the saturation function in the control law in order to avoid the chattering problem using the signum function, which is observed in Figure 4. For this case, torques t_1, t_2 are shown in Figure 5. Note that the chattering effect is eliminated using the saturation function, but the motion and force errors do not converge to zero, however they remain bounded. In Figure 6 we represent the module of force error in the constrained direction $\|e_{fc1}\|$ versus the module of motion error in the unconstrained direction $\|e_{xc2}\|$. We observe in this last figure that this trajectory, according to Equations 4.30 and pp. 11 of [14], remains ultimately bounded by

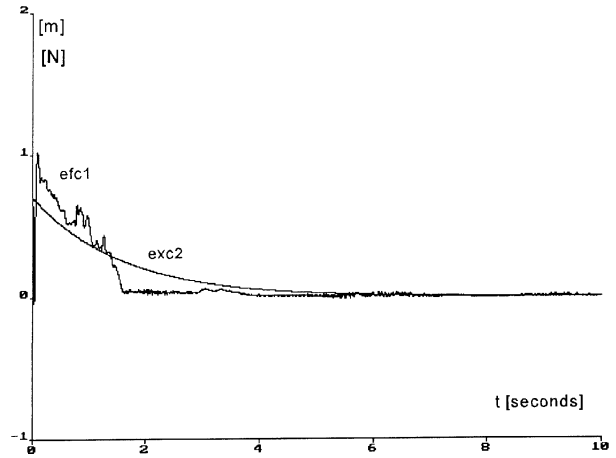

Figure 3. Force and motion error evolutions using the signum function.

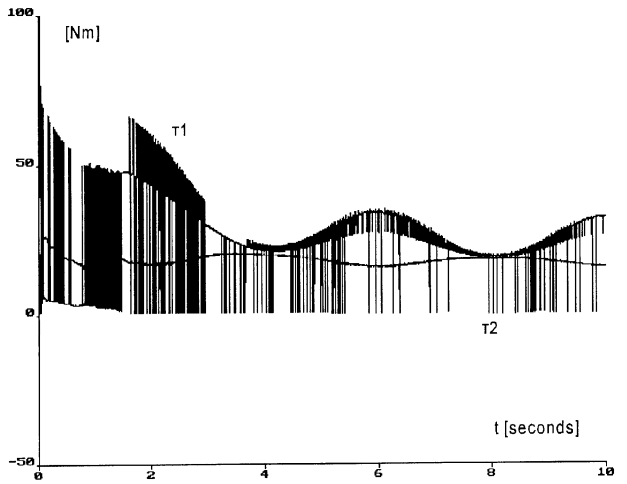

Figure 4. Control actions (applied torques) when using the signum function.

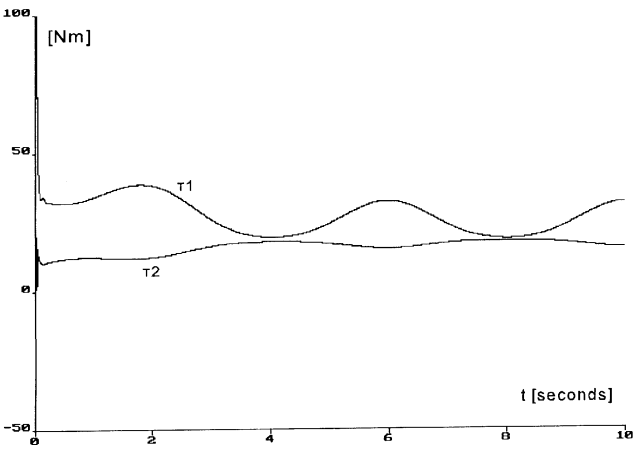

Figure 5. Control actions (applied torques) when using the saturation function.

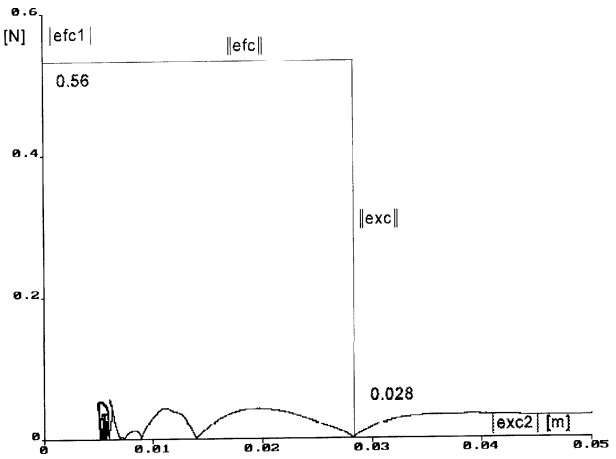

Figure 6. Force error module vs motion error module when saturation function is used.

$\| e_{mc} \| \le \| b_1 \| n_{mc} \| \le \| b_1 \| n_{mc} \|_2 = 0.028$ m and by

$\| e_{fc} \| \le \| b_3 k_e \| n_{fc} \| \le \| b_3 k_e \| n_{fc} \|_2 = 0.56$N.

CONCLUSIONS

In this paper, a robust hybrid motion/force controller for rigid link manipulators has been presented. Dynamic parameters and stiffness constant are assumed to be unknown but constant. The robust controller was shown to be globally stable in the sense that the control objectives are achieved asymptotically when signum function is used, occurring chattering effects. When we replace the signum function for a saturation function we avoid chattering problems and bounded motion and force errors are verified. The controller is based on a hybrid motion/force structure, including nonlinear feedback of joint position and velocities as well as the interactive force. Force derivative measurement is not necessary for this controller. Some simulation results for a two degree of freedom manipulator illustrate the controller performance.

ACKNOWLEDGMENT

This work was partially supported by CONICET - ARGENTINA.

REFERENCES

1. Spong M. W. and Vidyasagar M., "Robot Dynamics and Control", New York, John Wiley, (1989).
2. Whitney, D. E., "Historical Perspective and State of the Art in Robot Force Control", ***Int. J. Rob. Res.***, Vol. 6, (1987), 3-14.
3. Raibert M. H. and Craig J. J., "Hybrid Position/Force Control of Manipulators", ***ASME Trans. Dynam. Syst. J. Meas. Contr.***, Vol. 102, No. 2, (June 1981), 126-131.
4. Slotine J. J. and Li W., "Adaptive Manipulator Control: A Case Study", ***IEEE Trans. Automat. Contr.***, Vol. 33, No. 11, (Nov. 1988), 995-1003.
5. Kelly R. and Carelli R., "Unified Approach to Adaptive Control of Robotic Manipulators", ***Proc. of the IEEE-CDC***, Austin, TX, USA, (Dec. 1988), 1598-1603.
6. Ortega R. and Spong M., "Adaptive Motion Control of Rigid Robots: A Tutorial", ***Automatica***, Vol. 25, No. 6, (1989), 877-888.
7. Carelli R. and Kelly R., "Adaptive Hybrid Impedance/Force Controller for Robot Manipulators", ***Proc. of the 11th IFAC World Congress***, Tallin, Estonia, USSR, Vol. No. 9, (Aug. 1990), 274-279.
8. Abdallah C. et al., "Survey of Robust Control of Rigid Robots", ***IEEE Contr. Syst. Mag.***, Vol. 11, No. 2, (Feb. 1991), 24-30.
9. Spong M., "On the Robust Control of Robot Manipulators", ***IEEE Trans. Automat. Control***, Vol. 37, No. 11, (Nov. 1992), 1782-1786.
10. Yao B. and Tomizuka, M., "Robust Adaptive Motion and Force Control of Robot Manipulators in Unknown Stiffness Environments", ***Proc. of the IEEE-CDC***, San Antonio, Texas, (Dec. 1993), 142-147.
11. Anderson B. D. O. et al., "Stability of Adaptive Systems: Passivity and Averaging Analysis", The MIT Press, Cambridge, MA, (1986).
12. Hung J. Y., Gao, W. and Ung, J. C., "Variable Structure Control: A Survey", ***IEEE Trans. on Indust. Elec.***, Vol. 40, No. 1, (Feb. 1993), 2-22.
13. Desoer C. and Vidyasagar, M., "Feedback Systems: Input-Output Properties", Academic Press, (1975).
14. Vidyasagar M., "Nonlinear Systems Analysis", 2nd. Edition, Prentice Hall, 1993.
15. Astrom K. J. and Wittenmark, B., "Adaptive Control", 2nd. Edition, Addison-Wesley Publishing Company, Inc., (1995).
16. Sciavicco L. and Siciliano, B., "Modeling and Control of Robot Manipulators", The McGraw-Hill Companies, Inc., (1996).